Bias-Tuning and Modulation Characteristics of Transferred-Electron Oscillators

D. D. TANG, MEMBER, IEEE, AND RONALD J. LOMAX, SENIOR MEMBER, IEEE

Abstract—**A theoretical analysis of the tuning and modulation characteristics of transferred-electron oscillators is given. The effects of the device properties and temperature and the influence of the circuit are discussed. Experimental results are also reported.**

INTRODUCTION

An attractive property of GaAs transferred-electron oscillators is their capability of being operated over a wide frequency range. The oscillation frequency of the transferred-electron device operated in a circuit is determined by the condition that the susceptance of the device be matched by the susceptance of the circuit, which is a function of frequency only. Thus the oscillation frequency of the device can be changed by changing either the device susceptance or the circuit susceptance.

Transferred-electron devices have been built with structures, such as planar concentric [1], tapered [2], mesa, and three terminal [3]. Experimental results on the tuning characteristics of these structures were also reported [1]–[6]. Among these, only the mesa devices are used practically as microwave generators. Theoretical discussions of the tuning characteristics and mechanisms of mesa-structure devices can be made from two points of view. The first is based on the physical properties of a stable domain, such as the relation between the capacitance of the domain and the bias voltage [5]–[7]. The second is based on the device admittance calculated from a simpler device model [6], [8], [9]. These theories apply to the cases in which the dipole-domain growth time is short compared with the RF period, the minimum instantaneous voltage drops below threshold, and the domain length is short compared to the length of the diode. Only positive bias tuning, i.e., frequency increases as bias voltage increases, is predicted from those models.

The purpose of the present study is to give an improved understanding of the bias-tuning and modulation properties of X-band mesa-type transferred-electron devices. The tuning achieved by variation of the device susceptance and conductance was studied by means of a more complete device model which can simulate all of the operating modes and at various RF levels. The experimental results and theoretical calculations are both presented.

Manuscript received June 27, 1974; revised April 24, 1975. This work was supported by the Air Force Systems Command, Rome Air Development Center, under Contract F30602-74-C-0012.

D. D. Tang was with the Electron Physics Laboratory, Department of Electrical and Computer Engineering, University of Michigan, Ann Arbor, Mich. 48104. He is now with the IBM T. J. Watson Research Center, Yorktown Heights, N. Y. 10598.

R. J. Lomax is with the Electron Physics Laboratory, Department of Electrical and Computer Engineering, University of Michigan, Ann Arbor, Mich. 48104.

BIAS TUNING

Experimentally, it is found that the bias-tuning characteristics of transferred-electron oscillators are circuit dependent. The maximum operating bias voltage for most practical devices is approximately four times the threshold voltage for CW operation and slightly higher for pulsed operation. In this bias range the oscillation frequency and power may increase monotonically (called positive tuning in this paper), decrease monotonically (negative tuning), or increase to a maximum and then decrease as the bias voltage increases. The latter is observed most frequently. The bias voltage at which the frequency peak occurs is found to be different when the circuit load is changed, and there is a tendency for the output power to vary in the same way as the frequency. Discontinuity and hysteresis in both the frequency and power may also occur during tuning [10]. This discontinuity is frequently found to be accompanied by bias circuit oscillations. Nevertheless, relationships will be sought among the tuning characteristics, the device properties, and the circuit. The tuning characteristics of the oscillator and their relationship to the circuit have been investigated based on the results of a device simulation performed by solving the current continuity equation and Poisson's equation with a finite-difference method for a one-dimensional model of an n^+-n-n^+ device. It is assumed that the circuit is shorted at all the harmonic frequencies and therefore a sinusoidal RF voltage V_{RF} superimposed upon a dc bias voltage V_B exists across the device terminals. Thus the device can be characterized by its RF admittance, which is a function of V_B, V_{RF}, and f, the oscillation frequency. The velocity versus field relation used in the calculations is given by the expression

$$v = [\mu \mid E \mid + v_s(E/E_0)^4]/[1 + (E/E_0)^4] \qquad (1)$$

where

μ the low-field mobility;
v_s the saturation velocity;
E_0 4000 V/cm.

Values of μ and v_s as functions of temperature are given by Ruch and Fawcett [11]. The diffusion coefficient is assumed to be constant and equal to 200 cm^2/s. The details of the calculations have been described elsewhere [12].

Simulations were carried out for devices with flat doping-density profiles in the active region, $N_D = 10^{15}$ cm^{-3},

and length $l = 10.5$ μm. A doping notch is added at the cathode when a domain mode is simulated. Interest is focused on the properties of the device when it is operated near its maximum dc-to-RF conversion efficiency, i.e., operated slightly below its transit-time frequency and at an RF voltage $V_{RF} \simeq V_B - V_T$, where V_T is the threshold voltage. It was found that the traveling velocity of the space charge (either dipole domain or accumulation layer) is affected by the terminal voltage. A higher average velocity is found at a lower bias voltage. Similar results were reported in [13].

After a dipole domain is formed at the cathode, the front end of its depletion layer reaches the anode within approximately 50 ps. Therefore, for the device operating at X-band frequencies, quenching of the space charge by the down-swinging RF terminal voltage and collection of the space charge by the anode are both involved. The former becomes important in sustaining the coherent oscillation when the operating frequency is farther away from the transit-time frequency. Coherent oscillation can be maintained over a finite frequency range even when the instantaneous voltage does not swing below the threshold value. This tends to happen when the cathode doping notch is smaller and the bias voltage is high. Fig. 1 shows the current waveform of the accumulation mode operation. Fig. 2 shows the corresponding electric-field distribution. There is a stationary high field near the anode which accounts for most of the voltage drop. Due to the existence of this anode field, the minimum instantaneous field in the remainder of the device is below threshold even though the minimum voltage across the whole diode is above the threshold voltage. As a result, the space-charge injection angle is not fixed and is determined by the condition that the electric field at the cathode be above the threshold field. However, if the RF voltage is so large that the instantaneous voltage stays below threshold over part of the RF cycle, the space-charge region can be completely discharged. The new space charge is injected when the terminal voltage swings up above threshold.

A typical device admittance (domain mode) as a function of V_{RF} is shown in Fig. 3. The device conductance decreases as V_{RF} increases. Two different regimes are found in the device susceptance versus RF-voltage behavior. They can be characterized approximately by the condition that $V_{RF} > V_B - V_T$ and $V_{RF} < V_B - V_T$.

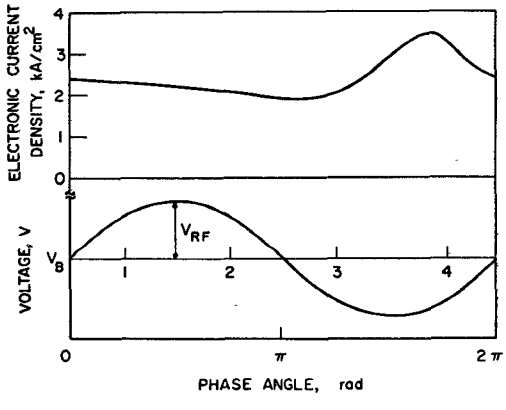

Fig. 1. Current and voltage waveforms for a TE device ($N_D = 10^{15}$ cm^{-3}, $l = 10.5$ μm, no cathode notch, $T = 300$ K, $V_B = 10$ V, $V_{RF} = 4$, $f = 14$ GHz).

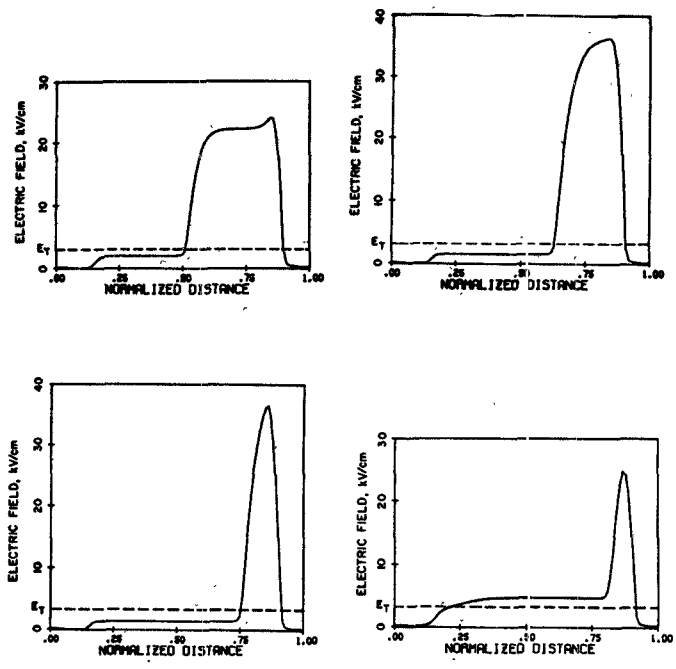

Fig. 2. Electric-field distribution at the four phase angles of Fig. 1. (a), (b), (c), and (d) correspond to phase angles 1, 2, 3, and 4, respectively.

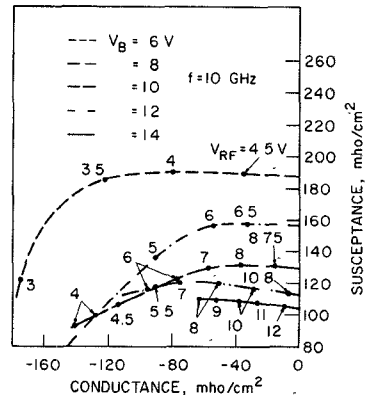

Fig. 3. Admittance of a TE device versus RF voltage ($N_D = 10^{15}$ cm^{-3}, $l = 10.5$ μm, $T = 300$ K, $f = 10$ GHz).

For the case $V_{RF} > V_B - V_T$, the instantaneous voltage swings below threshold each cycle. The device susceptance decreases very slowly with RF voltage and it decreases smoothly with the bias voltage. The time-average voltage drop across the dipole domain increases as the bias voltage increases. Thus the higher the bias voltage, the wider the domain and therefore the smaller the effective domain capacitance. When the domain width is comparable to the length of the active region of the device, its width is limited by this length; therefore the capacitance of the device tends to remain constant at high bias. The ratio of the device capacitance to the cold capacitance decreases from 6 to less than 3. Fig. 4 shows the ratio for the present calculations. In the same figures, the variation of the domain capacitance versus bias voltage calculated from the stable-domain model [6] is compared with the present results. The result is normalized with the present cal-

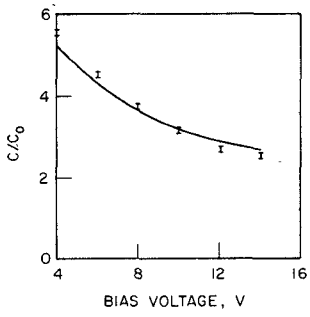

Fig. 4. Capacitance ratio versus bias voltage at 10 GHz for $V_{RF} > V_B - V_T$ ($N_D = 10^{15}$ cm^{-3}, $l = 10.5$ μm). Present results: I results from the stable-domain model of [6] ——.

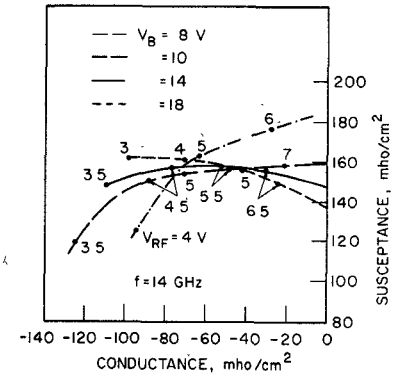

Fig. 5. Admittance of a TE device with the same structure as that of Fig. 3 but without a cathode notch. The dot on the constant bias admittance contour indicates where $V_{RF} = V_B - V_T$.

culation at $V_B = 8$ V. The close relationship between the domain capacitance and the device capacitance can be seen.

In the second RF-voltage regime, $V_{RF} < V_B - V_T$, the instantaneous voltage does not drop below threshold. There is an apparent phase shift between the RF voltage and the RF current compared with the first RF regime due to the shift in the injection angle. The device susceptance either increases or decreases as RF voltage decreases, depending on whether the frequency is higher or lower than the transit-time frequency, respectively. The change in device susceptance becomes more sensitive to the RF voltage when the operating frequency is farther away from the transit-time frequency. The amount of variation in device susceptance with respect to V_{RF} also depends on the bias voltage.

Similar results are found for the device operating in the accumulation-layer mode. However, the decrease in device susceptance with bias voltage is relatively smaller when the device is operated in the large RF-voltage regime. It is found that the traveling velocity of the accumulation layer is faster than that of the dipole domain under the same bias-voltage operation. Thus the transit-time frequency is higher. Fig. 5 shows the admittance of a device with the same structure but without a doping notch at the cathode. The device susceptance decreases as the bias voltage increases when the device negative conductance is small. This indicates that the device is operating in the large RF-voltage regime. At high bias in the large RF-voltage regime there is no negative conductance. At the smaller RF voltage, the device susceptance does not show the same kind of variation with the bias voltage. However, the border between the large and small RF-voltage regime is vague.

The device oscillation frequency shift Δf due to a change in device susceptance ΔB_d is

$$\Delta f/f = -(R/2Q)\,\Delta B_d \qquad (2)$$

where f is the oscillation frequency and R and Q are the circuit resistance and Q factor, respectively. The frequency decreases as the device susceptance increases. The operating point shifts along the circuit line as a result of the change in the bias voltage. From the analysis, the device total current is found to be contributed dominantly by the electronic current, not the displacement current. For example, the electronic current of an X-band diode (10 μm in length) is 8–10 times the displacement current in magnitude. Therefore the device susceptance is primarily controlled by the space-charge transit properties, not the cold capacitance. The total change in device susceptance ΔB_d can be written as

$$\Delta B_d = \frac{\partial B_d}{\partial f}\Delta f + \left[\left(\frac{\partial B_d}{\partial V_B}\right)\Delta V_B + \left(\frac{\partial B_d}{\partial V_{RF}}\right)\Delta V_{RF}\right]. \qquad (3)$$

When Δf is around tens of megahertz, the first term is very small compared with the remaining terms. The constant bias contour calculated for a fixed frequency would give a sufficiently good prediction of the bias-tuning characteristics. By assuming the circuit conductance to be constant for simplicity, the operating point susceptance and the RF power output as a function of the bias voltage can be found from the calculated device admittance. They are shown in Fig. 6. It is clear that the operating point susceptance is monotonically decreasing as the bias increases when the circuit conductance is low. According to (2), the device should show positive tuning. The magnitude of the frequency shift is inversely proportional to the circuit Q. The device susceptance shifts approximately 8 mmho for a change in bias from 6 to 14 V. This change of the device susceptance would give a shift of approximately 66 MHz in the frequency for a circuit with $Q = 200$. The maximum bias-tuning sensitivity occurs at the lower bias. When the operating point conductance is so large that the device is operated in the small RF-voltage regime, the bias-tuning characteristics have a peak in frequency at a certain bias. Above that bias voltage, the tuning in frequency is negative. The calculations also show that the bias voltage at which the device oscillates at the peak frequency tends to decrease as the operating point conductance increases. The tuning characteristic of the RF power is similar to that of the frequency. However, the peak in power does not necessarily occur at the same bias as the peak in frequency. Similarly, the tuning characteristics in a constant conductance circuit can be constructed for the device whose admittance is shown in Fig. 5. The device will show negative tuning in frequency in a high-conductance circuit and positive tuning in a low-conductance circuit (Fig. 7). The peak in power occurs at a lower bias voltage when the

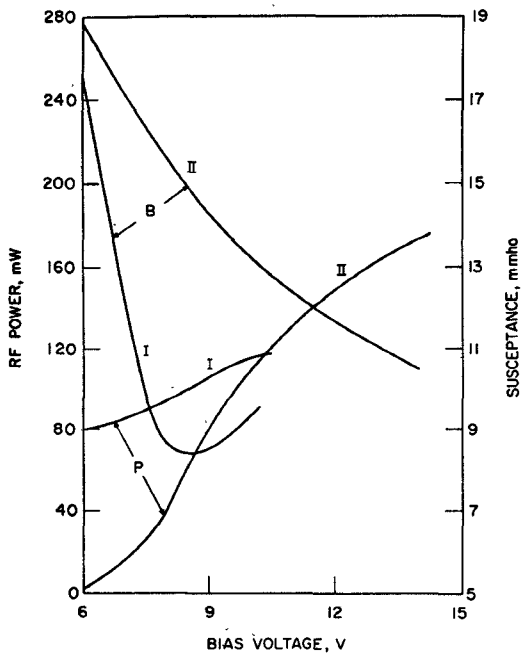

Fig. 6. Bias-tuning characteristic for a device with a cross-sectional area = 10^{-4} cm^2, $N_D = 10^{15}$ cm^{-3}, $l = 10.5$ μm, operated in a circuit with constant conductance (I: $G = 14$ mmho; II: $G = 3$ mmho).

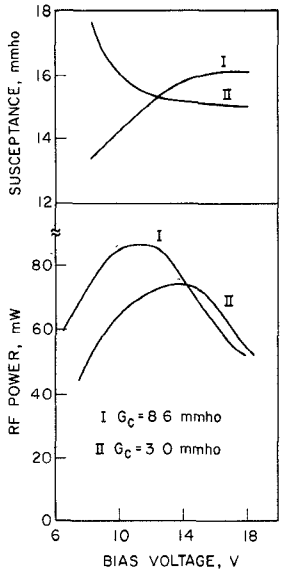

Fig. 7. Tuning characteristics of a device in the accumulation-layer mode ($N_D = 10^{15}$ cm^{-3}, $l = 10.5$ μm, $A = 10^{-4}$ cm^2, $T = 300$ K, $f = 14$ GHz).

circuit conductance is higher. Such tuning characteristics should be seen in the low doping-density-length product device because the device is unlikely to form a dipole domain [13]. Devices operated CW may also show such tuning characteristics because of the reduction of the low-field mobility and the peak-to-valley ratio of the velocity-field relation, which slows down the growth of the space charge.

So far, the bias-tuning characteristics have been discussed for a device in a constant conductance circuit. The microwave resonant cavity is generally a multiply resonant circuit. The circuit conductance varies with the frequency. As a result, the tuning characteristics discussed here should be modified due to the variation of the operating point conductance with frequency.

Experimentally, changes in circuit load seen by the oscillator can be achieved by changing the coupling iris of the waveguide cavity in which the transferred-electron oscillator is mounted. The resonant frequency of the cavity can be maintained nearly constant. The circular window iris of thin gold-plated copper acts as a shunt inductor between the load and the cavity [14]. An iris with a smaller diameter couples less external load to the cavity. Several diodes were tested in this circuit and their tuning characteristics are similar. Generally, continuous bias tuning is difficult to obtain without encountering bias circuit oscillations when a large diameter iris is used. A typical result is shown in Fig. 8. It is clear that the peaks of frequency and power tend to occur at higher bias as the circuit load is reduced. The device tested has been analyzed with an empirical equivalent circuit [15]. The circuit conductance around the operating point is approximately 3.8 and 1 mmho for iris diameters of 0.25 and 0.20 in, respectively. The RF voltage is estimated on the basis of the method described in [15] and is shown in the same figure. The decrease of the dc current is partially due to the increase of the RF level of the oscillation [12] and partially due to the increase of the device temperature. A noisy spectrum is frequently seen in the negative tuning portion for bias above 10.5 V. The exact reason is not clear; it may be caused by avalanche in the anode high-field region. The effects of temperature on the device operating frequency are obtained by comparing the frequency shift data from the dc pushing and pulse pushing (pulse superimposed on constant dc) for operation of device number 2 in the waveguide cavity. Fig. 9 is a plot of frequency shift versus bias voltage. Curve I shows dc pushing and curve II shows pulse pushing for a dc bias of 10 V. The temperature increases with the bias voltage for each point along curve I. Curve II is a constant temperature curve. At the crossover point, i.e., 10 V, the curves are at the same temperature and the

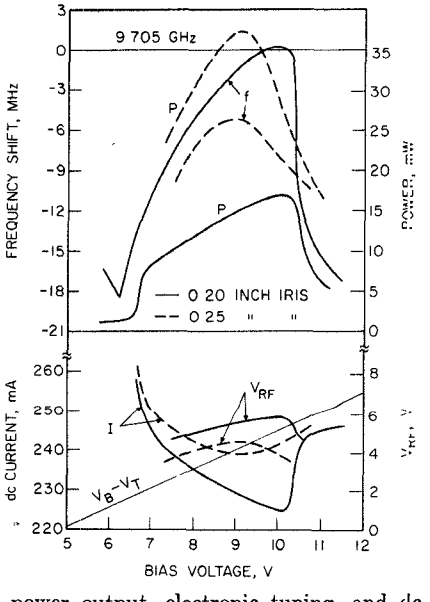

Fig. 8. RF power output, electronic tuning, and dc current for device number 2 in the waveguide cavity.

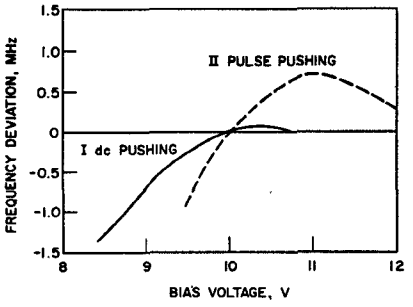

Fig. 9. Dc and pulse-pushing measurements for device number 2. The device is operated at $f_0 = 9.086$ GHz in a waveguide cavity with a 0.25-in-diam iris.

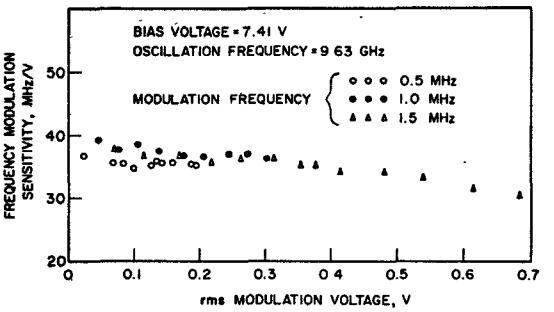

Fig. 10. Frequency modulation sensitivity versus rms modulation voltage of Gunn device in a coaxial cavity ($V_T = 4.4$ V, $I_T = 0.105$ A).

same frequency. It is clear that the frequency drops as the temperature increases. From the device resistance [11] as a function of heat-sink temperature at low bias, the thermal resistance is estimated to be approximately 52°C/W. The temperature change of the device between 9.5 and 10.0 V is approximately 7°C. By comparing the two curves at 9.5 V, it is found that the frequency decreases at a rate of approximately 0.1 MHz/°C in this circuit. This indicates that for narrow-range frequency modulation the temperature effect is significant [16]. However, the general tuning characteristic is not dictated by the temperature.

BIAS MODULATION

Bias modulation is achieved by modulating the bias voltage so that $V_B = V_{dc} + F(t)$, where $F(t)$ is the modulating signal. In this study a sinusoidal modulating signal is utilized to investigate the modulation sensitivity, linearity, and the modulation bandwidth of transferred-electron devices. When the modulating frequency is low, the bias modulation can be treated essentially the same way as bias tuning, i.e., the operating point admittance shifts up and down along the circuit line at the modulating frequency f_m. The frequency modulation sensitivity [6] is proportional to the frequency range on the circuit line intersected by the constant bias device admittance lines. Similarly, the amplitude modulation sensitivity is proportional to the power range on the constant bias device lines intersected by the circuit line. From Figs. 6 and 7 it can be predicted that a larger modulation sensitivity is obtained at a lower bias voltage. Such results should be found in both positive and negative tuning regimes. To obtain linear modulation over a wide range, a proper operating point must be chosen. Experimentally, the Bessel null method [6] can be utilized to measure the frequency modulation sensitivity. However, analyses [12] show that the accuracy of the Bessel null method is affected by the existence of AM in the FM signal. Fig. 10 shows the frequency modulation sensitivity versus modulation frequency for an operating point where AM is less than 1 percent. The modulation sensitivity is independent of the modulation frequency and decreases very slowly when the modulation voltage is large. More detailed experimental results are given in [6].

The modulation bandwidth is the upper limit of the modulating signal frequency. Since AM and FM are usually coexistent, it is believed that the limit is related to the relaxation time of the RF amplitude of the oscillator. The exact modulation bandwidth is determined by the detailed relations between circuit admittance as a function of frequency and the device admittance as a function of V_{RF}. For simplicity, the circuit conductance G_c is assumed constant and the frequency shift is small compared with the operating frequency. It is also assumed that the transition time is much longer than the period of the RF oscillation. The following is obtained from the power balance between the oscillator and the circuit:

$$P_d = P_c + \frac{dW_c}{dt} \tag{4}$$

where P_d is the power generated by the active device, P_c is the power dissipated by the circuit conductance, and dW_c/dt is the time variation of the energy stored in the system. In terms of V_{RF}, P_d, P_c, and W_c can be expressed as $(1/2) \mid g_d \mid V_{RF}^2$, $(1/2)G_cV_{RF}^2$, and $(1/2)(Q/\omega)G_cV_{RF}^2$, respectively, where Q is the circuit Q factor and $\omega = 2\pi f$ is the radian frequency of RF oscillation.

(Q/ω) is approximately equal to a constant based on the assumption that the frequency shift is small compared with the oscillation frequency. After substituting these relations into (4) and with some manipulation the following is obtained:

$$\frac{dV_{RF}}{dt} = \frac{\omega}{2Q} V_{RF}\left(\frac{\mid g_d \mid}{G_c} - 1\right) \tag{5}$$

or

$$\Delta t = \frac{2Q}{\omega}\int_{V_i}^{V_i+\Delta} \frac{dV_{RF}}{V_{RF}(\mid g_d \mid /G_c - 1)} \tag{6}$$

where Δt is the transition time for V_{RF} to change from V_i to $V_i + \Delta$. V_i is the RF voltage of the initial state and Δ is $0.9 \cdot (V_f - V_i)$, where V_f is the RF voltage of the final state. The transition time is directly proportional to the factor Q/ω and is determined by $\mid g_d \mid$. Assume under constant bias voltage that $\mid g_d \mid = (g_0/V_{RF})$, where g_0 is a function of bias voltage. The Δt for a step change in bias voltage (the device admittance) can be obtained by integrating (6). The result is

$$\Delta t = 4.6\frac{Q}{\omega}. \tag{7}$$

For a typical resonant circuit with $Q = 200$, the transition time is 14.6 ns when the oscillation frequency is 10 GHz. Thus it is 146 times longer than the RF period. The corresponding modulation bandwidth is

$$f_m|_{\max} \simeq \frac{1}{\Delta t} \simeq 70 \text{ MHz}.$$

Within this modulation bandwidth any modulation can be considered as the same as bias tuning. When the modulating signal is close to and above this bandwidth, the modulation sensitivity is expected to decrease. It is noted that (7) is computed under the assumption $|g_d| = (g_0/V_{RF})$. For devices with different g_d versus V_{RF} characteristics, the transition time will be different.

CONCLUSIONS

The tuning and modulation properties of transferred-electron devices have been described. The device behavior was characterized by its RF admittance which was calculated from a large-signal analysis. The bias-tuning characteristics were predicted from the device RF admittance. The tuning characteristics of the device, the circuit load, and the circuit Q factor are interrelated. Experimental results were also given and compared with the analysis. The modulation bandwidth was found to be determined by the circuit Q factor, the oscillation frequency, and the device-admittance versus RF-voltage relationship. Within this modulation bandwidth, the bias-modulation properties can be derived from the bias-tuning characteristics. The modulation sensitivity is independent of the modulating frequency, but changes with bias voltage.

ACKNOWLEDGMENT

The authors wish to thank Dr. W. R. Curtice and Prof. G. I. Haddad for valuable discussions concerning this work.

REFERENCES

[1] B. Jeppsson, I. Marklund, and K. Olsson, "Voltage tuning of concentric planar Gunn diodes," *Electron. Lett.*, vol. 3, pp. 498–500, Nov. 1967.
[2] M. Shoji, "A voltage tunable Gunn-effect oscillator," *Proc. IEEE* (Lett.), vol. 55, pp. 130–131, Jan. 1967.
[3] K. G. Petzinger, A. E. Hahn, Jr., and A. Matzelle, "CW three-terminal GaAs oscillator," *IEEE Trans. Electron Devices* (Corresp.), vol. ED-14, pp. 403–404, July 1967.
[4] I. B. Bott, C. Hilsum, and B. C. Taylor, "Amplitude and frequency modulation of transferred electron microwave generators," *IEEE Trans. Electron Devices* (Corresp.), vol. ED-13, pp. 193–194, Jan. 1966.
[5] G. King and M. P. Wasse, "Frequency modulation of Gunn-effect oscillators," *IEEE Trans. Electron Devices* (Corresp.), vol. ED-14, pp. 717–718, Oct. 1967.
[6] W. C. Tsai and F. J. Rosenbaum, "Amplitude and frequency modulation of a waveguide cavity CW Gunn oscillator," *IEEE Trans. Microwave Theory Tech. (Special Issue on Microwave Circuit Aspects of Avalanche-Diode and Transferred Electron Devices)*, vol. MTT-18, pp. 877–884, Nov. 1970.
[7] W. E. Wilson, "Domain capacitance tuning of Gunn oscillators," *Proc. IEEE* (Lett.), vol. 57, pp. 1688–1690, Sept. 1969.
[8] D. D. Khandelwal and W. R. Curtice, "A study of the single-frequency quenched-domain mode Gunn-effect oscillator," *IEEE Trans. Microwave Theory Tech.*, vol. MTT-18, pp. 178–187, Apr. 1970.
[9] T. Ikoma and H. Yanai, "Effect of external circuit on Gunn oscillation," *IEEE J. Solid-State Circuits*, vol. SC-2, pp. 108–113, Sept. 1967.
[10] K. Kurokawa, "Some basic characteristics of broadband negative resistance oscillator circuits," *Bell Syst. Tech. J.*, vol. 48, pp. 1937–1955, July/Aug. 1969.
[11] J. G. Ruch and W. Fawcett, "Temperature dependence of the transport properties of gallium arsenide determined by a Monte Carlo method," *J. Appl. Phys.*, vol. 41, pp. 3843–3849, Aug. 1970.
[12] D. Tang, "Theoretical and experimental studies of the tuning and modulation properties of transferred-electron devices," Ph.D. dissertation, Univ. Michigan, Ann Arbor, 1974.
[13] D. E. McCumber and A. G. Chynoweth, "Theory of negative-conductance amplification and of Gunn instabilities in 'two-valley' semiconductors," *IEEE Trans. Electron Devices (Special Issue on Semiconductor Bulk-Effect and Transit-Time Devices)*, vol. ED-13, pp. 4–27, Jan. 1966.
[14] N. Marcuvitz, *Waveguide Handbook*. New York: Dover, 1965, pp. 408–409.
[15] W. R. Curtice, "Quenched-domain mode oscillation in waveguide circuits," *IEEE Trans. Microwave Theory Tech.*, vol. MTT-21, pp. 369–374, June 1973.
[16] B. A. E. De Sa and G. S. Hobson, "Thermal effects in the bias circuit frequency modulation of Gunn oscillators," *IEEE Trans. Electron Devices*, vol. ED-18, pp. 557–562, Aug. 1971.

Short Papers

The Method of Series Expansion in the Frequency Domain Applied to Multidielectric Transmission Lines

A. F. DOS SANTOS AND J. P. FIGANIER

***Abstract*—In this short paper a method of expanding the phase constant and the field of a multidielectric transmission line as a power series of the frequency is developed. The method provides a theoretical justification for the widely used "static" approximations and indicates the reason why their accuracy is frequently good. This expansion may also be useful for estimating an upper limit to the frequency band in which the dispersion does not exceed a specified value. A numerical example is included.**

Manuscript received January 6, 1975; revised April 15, 1975.

The authors are with the Complexo Interdisciplinar, Instituto Superior Técnico, Lisbon, Portugal.

I. INTRODUCTION

Most practical strip transmission lines are structures in which two dielectrics are present, one being air and the other a solid insulator having small losses in the operating frequency range. The solid dielectric has an electric permittivity different from that of air and therefore TEM modes cannot propagate. Independent TE and TM modes are seldom possible, and in consequence, the propagating modes in all practical two-dielectric strip lines are hybrid.

For the usual mode of operation, the lowest order one, the wave equation tends to the two-dimensional Laplace equation as the frequency tends to zero and hence the axial components should be small compared with the transverse ones for sufficiently low frequencies, making this mode almost TEM. Interest thus arises in the characteristics obtained from static fields, namely a phase constant $\beta = \omega(LC)^{1/2}$ and a characteristic impedance $Z_0 = (L/C)^{1/2}$, where L and C are, respectively, the inductance and capacitance per unit length.

In the following sections a method of field expansion as a power